Process Biochemistry 47 (2012) 1327–1334

Contents lists available at SciVerse ScienceDirect

Process Biochemistry

journal homepage: www.elsevier.com/locate/procbio

Synthesis and sorption performance of highly specific imprinted particles for the direct recovery of carminic acid

Noor Shad Bibi[a], Leonardo Galvis[a], Mariano Grasselli[b], Marcelo Fernández-Lahore[a,*]

[a] Downstream BioProcessing Laboratory, School of Engineering and Science, Jacobs University, Campus Ring 1, D-28759 Bremen, Germany
[b] Laboratorio de Materiales Biotecnológicos, Depto. de Ciencia y Tecnología, Universidad Nacional de Quilmes, Roque Sáenz Peña 352 (B1876BXD) Bernal, Argentina

ARTICLE INFO

Article history:
Received 26 July 2011
Received in revised form 19 April 2012
Accepted 27 April 2012
Available online 19 May 2012

Keywords:
Molecularly imprinted polymer, Carminic acid, Finite bath adsorption, Solid phase extraction, Langmuir–Freundlich isotherm

ABSTRACT

Carminic acid (CA) is a colorant of natural origin, which is demanded by the food, cosmetic, and pharmaceutical industries. In this work, a selective finite bath process was developed based on the utilization of molecularly imprinted polymeric particles. Such adsorbent was synthesized in a (porous) particle shaped form employing methacrylic acid (MAA) and 4-vinylpyridine (4Vpy) as monomers and ethylene glycol dimethacrylate (EDGMA) as a cross-linker. The imprinted particles were characterized by surface area, surface charge and pore size determination. The adsorption behavior of CA on such a material followed a Langmuir–Freundlich isotherm. Maximum capacity at equilibrium reached 0.64 mmol/g (316 mg/g) and maximum available binding sites 1.8 mmol/g (917 mg/g) were observed for an association coefficient value of 1.5 mM^{-1}. Further, the imprinting factor; showing the strength of interaction of CA to the polymer, was calculated as 13 while the selectivity factor depicted a value of 15. The data presented indicates that the imprinted adsorbent could be conveniently utilized for the recovery of CA, from cochineal extract, in the finite bath mode of operation.

1. Introduction

Color is an extremely important sensory characteristic of food. Color additives reinforce colors in the food and ensure its uniformity. Fat-soluble synthetic colors are class III carcinogens by the International Agency for Research on Cancer (IRAC) [1]. Some of the water-soluble dyes, such as Amaranth, Fancy red and Ponceau 4R are allowed but the allowable amount and extent of utilization are strictly restricted in foodstuff in various countries [2]. Throughout the world, the use of natural type food colors continues to increase. Many consumers perceive the natural colors as less harmful and thus most acceptable [3].

Carminic acid (E 120) is a natural red dye extracted from cochineal, the desiccated bodies of female *Dactylopius coccus* Costa insects. Carminic acid is neither toxic nor known to be carcinogenic. However, impure dye preparations may induce allergic reactions in a sub-group of susceptible individuals within the general population. Carminic acid solutions prepared with water have little intrinsic color below pH 7, where the quinine ring has greatest photo stability and these solutions are a pale-straw tint at pH near 4 [4]. Due to its fugitive nature, carmine is now principally used in the food, cosmetic, and pharmaceutical industries [5].

The recovery and purification of carminic acid from raw cochineal is regarded as a difficult and complicated process. The colorant is normally isolated by a precipitation with bivalent ions [5] but it was recently demonstrated that sequestration on beaded adsorbents is a viable industrial strategy [4,6]. However, for products of natural origin the cost of the adsorbent is a key issue. Batch contacting at process scale offers the opportunity to exploit cheaper materials whose lack of geometric refinement and/or lack of inherent particle density make them unsuited for fixed- or fluidized-bed applications [4]. However, the main drawback associated with such sorbents is the lack of selectivity, which introduces the need for extensive optimization of the process conditions and parameters [7].

Materials with high adsorption capacity and selectivity toward particular (targeted) species are in demand. Traditionally, sorption performance has been attempted by physical or chemical modification to the material surface. Recent research has shown the potential of the molecular imprinting technique (Molecularly Imprinted Polymers/MIPs) to confer appropriate selectivity to adsorbents in various formats. The MIP approach has been already applied to exert the selective separations of organic compounds [8]. Wulff and Sarhan introduced MIPs in 1972 [9] while Arshady and Mosbach introduced the so-called non-covalent approach in 1980s. The target molecule is used as a template for imprinting cross-linked polymers. After removal of the template, the remaining polymer is more selective for the target molecule as compared to non-imprinted one; the selectivity depends on the size and shape

* Corresponding author. Tel.: +49 421 200 3239; fax: +49 421 200 3600.
E-mail address: m.fernandez-lahore@jacobs-university.de (M. Fernández-Lahore).

1359-5113/$ – see front matter © 2012 Published by Elsevier Ltd.
http://dx.doi.org/10.1016/j.procbio.2012.04.030

Nomenclature

k	retention factor
I_f	imprinting factor
N_i	number of binding sites at certain K_i (mmol/g)
K_i	affinity constant having N_i binding sites (mM^{-1})
K_0	affinity constant (mM^{-1})
α	related to median binding affinity; $K_0 = \alpha^{1/m}$ (mM^{-1})
m	heterogeneity index
B	concentration of bound template at equilibrium (mmol/g)
F	concentration of free template at equilibrium (mM)
N_t	total number of binding sites (mmol/g)
c_0	initial liquid phase concentration (mM)
w	mass of beaded adsorbent (g)
ν	kinematic viscosity (St)
V	volume of liquid (L)

of the cavity. Association and dissociation of the template to the MIP takes place without requiring any covalent interaction and the template only diffuse in and out of the complementary sites [10]. Usually the MIP is used for detection purpose [11], here it is preferred to use for the purification of huge amount of the products.

The goal of this work was to synthesize a highly specific imprinted polymer for carminic acid in the form of irregular particles, to characterize such an adsorbent, and to evaluate its performance for the sequestration of the mentioned dye in a finite bath operation.

2. Theory

2.1. Sorption at equilibrium

An adsorption isotherm describes the relationship of the concentrations of an adsorbate on a solid vs. the concentration of such entity in a liquid phase, in contact with the mentioned solid, at equilibrium and at constant temperature. Since MIP adsorbents are usually heterogeneous, estimation of binding properties is performed relying on the generalization that at low guest (adsorbate) concentrations, the contributions of the high affinity binding sites can be evaluated, and at high guest (adsorbate) concentrations, the contributions of the low-affinity sites can be assessed.

The Langmuir–Freundlich (LF) isotherm (also known as the Sips equation) [12], is a function that describes a specific relationship between the equilibrium concentration of bound (B) and free (F) guest in heterogeneous systems with three fitting coefficients according to:

$$B = \frac{Nt\alpha F^m}{1 + \alpha F^m} \tag{1}$$

where F is the concentration of template in solution (mM), B is the concentration of template in polymeric material (mmol/g), N_t is the total number of binding sites (mmol/g), α is a variable related to the median binding affinity (K_0) via $K_0 = \alpha^{1/m}\,mM^{-1}$, and m is the heterogeneity index, which varies from 0 to 1; values of $m < 1$ indicate that the material has a multiplicity of different binding sites.

The LF model has the advantage that it does not require an independent measure of the total number of binding sites (Nt), which is very difficult to measure in heterogeneous MIPs [13]. The difference between the LF model and the Freundlich equation is that at high adsorbate concentrations the LF model is able to represent a saturation behavior; at low adsorbate concentrations, the (LF) equation reduces to the classical Freundlich equation. On the other hand, as m approaches unity i.e. indicative of a completely homogeneous surface (or energetic equivalence of all binding sites) the LF model reduces to the classical Langmuir equation. Thus, the hybridized LF isotherm is able to model adsorption of solutes at high and low concentrations onto homogeneous and heterogeneous materials [14].

The affinity (or energetic) distribution of solute adsorption on MIP materials provides information on the heterogeneity of the adsorption sites within the polymeric structure [15]. The affinity distribution is represented as a plot of N_t (number of binding sites) vs. K_i (the association constants). In this way, a quantitative measure of the number of binding sites with respect to the corresponding binding affinity can be obtained, as well as, the breadth of the heterogeneity phenomenon. The general function for affinity distribution for the LF binding model can be written in the form:

$$N_i = N_t am \left(\frac{1}{K_i}\right)^m \frac{1 + 2a(1/K)^m + a^2(1/K_i)^{2m} + 4a(1/K_i)^m m^2 - a^2(1/K_i)^{2m} m^2 - m^2}{(1 + a(1/K_i)^m)^4} \tag{2}$$

This expression allows for the calculation of the number of binding sites (N_i) having an association constant value (K_i) by utilizing three fitting parameters (a, m, N_t) [13].

2.2. Sorption kinetics in finite bath

The kinetic rate constant model is based on the definition of an apparent adsorption rate constant, as a single adjustable parameter (k_1). Thus, the model takes an empirical approach to the adsorption process and assumes that the entire rate-limiting processes can be represented by kinetic rate constants. In such approach, the rate of mass transfer of the adsorbate to the solid support is described by the following equation:

$$C = C_0 - \frac{\nu}{V_0}\left[\frac{(b-a)(1 - \exp\{-((2aw/V)k_1 t)\})}{((b-a)/(b-a))(1 - \exp\{-((2aw/V)k_1 t)\})}\right] \tag{3}$$

$$a^2 = b^2 - \left(\frac{c_0 V}{\nu}\right) q_m \tag{4}$$

$$b = \frac{1}{2}\left(\frac{c_0 V}{\nu} + q_m + \frac{K_d V}{\nu}\right) \tag{5}$$

where c_0 is the initial liquid phase concentration (mM), w is the mass of beaded adsorbent (g), ν is the kinematic viscosity and V is the volume of liquid external to the adsorbent. The parameters N_t and K_0 are obtained by non-linear regression of the LF isotherm. The apparent adsorption rate constant approach was successfully undertaken by us and other authors to evaluate the kinetics of industrial relevant systems [4,6].

3. Material and methods

3.1. Materials

Ethylene glycol dimethacrylate (EGDMA), 4-vinylpyridine (4Vpy), dimethylsulfoxide (DMSO) and methacrylic acid (MAA) were obtained from Sigma–Aldrich (Steinem, Germany). 2,2-Azobis (2-isobutyronitrile) (AIBN) was from Fluka (Steinem, Germany). Erythrosine B (C.I. 45430) was purchased from Merck (Darmstadt, Germany). Carminic acid (C.I. 75470), in a highly purified form, was kindly donated by Naturis SA (Buenos Aires, Argentina). MAA and 4Vpy were purified by distillation under reduced pressure. All other reagents were used as received.

3.2. Methods

3.2.1. Polymer synthesis

The MIP adsorbent particles were synthesized by the bulk polymerization technique utilizing MAA and 4Vpy as monomers (M) in the presence of EDGMA as a cross-linker (CL). Carminic acid was employed as the template. Briefly, CA (0.081 mmol) was mixed with the monomers (0.93 mmol); the mixture was kept

for 1 h at room temperature. Subsequently, EGDMA (4.66 mmol) was added to the reaction mixture, which was kept for additional 4 h at 24 °C. Finally, 10 mg of AIBN (as initiator) and 1.27 ml of DMSO (as porogen) were incorporated, the mixture was purged with nitrogen for 10 min, the reaction tube was sealed, and the polymerization let to proceed at 60 °C for 16 h. The resulting solid (5 g) was crushed and sieved to obtain a defined cut of particle sizes (25–71 μm). The removal of the template was done by repeated washes with ethanol (70%) followed by Soxhlet extraction with 200 ml of absolute ethanol. Washed particles were dried at 80 °C for 24 h. Non-imprinted particles, which were utilized in control experiments, were synthesized following exactly the same procedure but in the absence of a CA as a template. The so-called MV_{MIP} was prepared utilizing a mixture of MAA and 4-Vpy as monomers while the V_{MIP} was synthesized employing only 4-Vpy as a monomer.

3.2.2. Physical characterization of polymers

The pore size and surface area of the MIP particles were determined by nitrogen adsorption in a Nova Win V 1.12 (Quantachrome, Odelzhausen, Germany), employing the Brunauer, Emmer and Teller (BET) equation. The adsorption isotherms were measured using 40 point pressure table. The pore size distribution was determined utilizing BJH model.The particle zeta potential was measured employing a Zetasizer Nano ZS (Malvern Instruments, Worcestershire, UK). Particles of MIP were suspended in 50 mM ammonium acetate buffer solution (pH 4) or in a 20 mM phosphate buffer solution (pH 7.6) and the suspension diluted to appropriate particle count (≈200) before taking the measurements. Zeta potential values were calculated from electrophoretic mobility data according to Smoluchowski's equation [16].

3.2.3. Screening of MIP materials

A screening assay was developed in order to obtain material leads for further evaluation. Briefly, MIP particles were contacted with an aqueous solution of CA (1.25 mg/ml, pH 4) for 2 h at room temperature under gentle stirring. The solid to liquid phase ratio was 10. After contacting, the particles were extensively washed with distilled water and the adsorbed CA was eluted with a 0.5 N sodium hydroxide solution. Commercial adsorbent resin beads, as well as NIP particles were utilized as controls. For this purpose 200 μl of aqueous solution, containing 1 mg/ml CA was contacted with 20 mg of the material. After 2 h, the decrease in the supernatant concentration of CA was determined and the amount of CA bound was calculated. The same buffer performed washing 3 times and then CA was recovered by 0.5 M NaOH.

3.2.4. Equilibrium adsorption characteristics

3.2.4.1. Adsorption isotherms. Adsorption isotherm experiments were performed in 1.0 ml Eppendorf tubes. Briefly, 20 mg of MIP particles (or non-imprinted/NIP particles as a control) were deposited in a series of 10 tubes. Subsequently, 200 μL of a CA solution was added (concentration range from 4.0 to 40 mg/ml), and the tubes were gently mixed by inversion for 16 h. Particles were separated by gravity settling (30 min) and the CA concentration in the supernatant was measured as described in Section 3.2.6. From this data, the amount of adsorbed CA was calculated. Data were fitted using non-linear regression methods utilizing a program (Graph Pad Prism, San Diego, CA, USA) employing the Langmuir–Freundlich equation.

3.2.4.2. Affinity distribution. To characterize the heterogeneity of the adsorbents, the affinity distribution of the MIP particles was calculated according Umpleby et al. [17]. Affinity distribution was defined as number of binding sites observed as a function of the corresponding association constant values. The number of binding sites at a specific association constant value (K) was calculated by inserting the parameters m and α (from Langmuir–Freundlich isotherm) to Eq. (2). The minimum value (K_{min}) and the maximum value (K_{max}) for the association constant were calculated as $K_{min} = 1/F_{max}$ and $K_{max} = 1/F_{min}$, respectively; F is the free concentration of template in the adsorption experiments.

3.2.5. Selectivity of the imprinted particles

The selectivity of the MIP particles was evaluated by chromatographic experiments. In doing so, MIP particles (or NIP particles for control experiments) with an average diameter ≈ 50 μm were packed in a 100 mm × 5 mm column (Tricorn, GE Healthcare, Munich, Germany). Isocratic experiments were performed at a BioCAD 700 E Workstation (Applied Biosystems, Foster City, CA, USA). The mobile phase was prepared by mixing 7 parts of 50 mM acetate buffer (pH 4) with 3 parts of organic modifier (1 part of methanol and 1 part of acetonitrile). The flow rate was 1.0 ml/min. Samples (200 μl; 1.0 mg/ml) containing either carminic acid or the structural analog Erythrosine B were injected into the system and the retention time (t_R) measured by UV/VIS monitoring at 494 nm and 525 nm, respectively. Zero retention (t_0) was measured employing 2% acetone as a tracer and UV detection at 280 nm. The retention factors (k) were calculated according to the equation:

$$k = \frac{t_R - t_0}{t_0} \quad (6)$$

The values of the retention factors in the template and its structural analog were utilized to calculate the imprinted factor (I_f) and the selectivity factor (S_f), according to:

$$I_f = \frac{k_{MIP}}{k_{NIP}} \quad (7)$$

$$S_f = \frac{k_{MIP\text{-}TEMPLATE}}{k_{MIP\text{-}ANALOG}} \quad (8)$$

Where $k_{MIP\text{-}TEMPLATE}$ and $k_{MIP\text{-}ANALOG}$ are the retention factors for MIP while the samples were carminic acid and the structural analog (Erythrosine B) respectively.

3.2.6. Adsorption performance in a finite bath

The cochineal extract was extracted according to standard industry practices, as proposed by Cabrera and Fernandez-Lahore [6]. Briefly, 10 g of finely ground cochineal was treated with 50 ml sodium hydroxide (0.15 M) at 90 °C for 20 min. The mixture was subsequently diluted with 150 ml of hot distilled water and heated for additional 20 min with stirring. The extract was then filtered using cheese cloth so as to remove coarse cochineal fragments, the pH of the filtrate was adjusted to 4.0, and the extract was further clarified by centrifugation (3000 × g). The concentration of carminic acid was determined utilizing the method recommended by the joint FAO/WHO expert committee on food additives, modification proposed by Cabrera and Fernandez-Lahore [6]. A value of 5800 was taken for the molar adsorptive coefficient of carminic acid (ε @ 494 nm) in a 0.02 N chloridric acid solution.

Finite bath experiments were performed in a stirred tank with a total volume of 500 ml, and a 9.0 cm internal diameter; the vessel aspect ratio was 2. A paddle type impeller (4.0 cm diameter) was utilized. The dimensionless concentration of CA was measured against time at varying impeller velocities (56, 156, 256 and 356 rpm). The total adsorbent load was 5% (w/v). 500 μL samples were taken at different time intervals for carminic acid determination. Data were plotted as normalized concentration as a function of process time.

4. Result and discussion

The aim of this project was the recovery of carminic acid from raw cochineal extract. Adsorption was supposed to be the most favorable approach for this recovery. Highly specific beaded particles (imprinted polymers) were synthesized, utilizing a commercially available pure carminic acid as a template for the synthesis. The particles were subjected to various characterizations and finally the raw cochineal extract was applied to observe the direct recovery from the solution.

4.1. Polymer synthesis

Molecularly imprinted polymers have been developed for numerous applications but studies on materials with recognition properties toward dyes are rather few [18]. In this work carminic acid (red dye) was utilized as a template for MIP synthesis. Carminic acid is an anthraquinon glycoside containing several acidic centers; this includes a carboxylic group (pK_a 2.9). Fig. 1 depicts the chemical structure of carminic acid and the structural analog (Erythrosine B).

Considering the potential ability of the template to establish either ionic interactions or hydrogen bonding in polar media; two readily available monomers, MAA and 4Vpy, were selected for polymer synthesis. Although MIP materials are typically prepared using non-polar solvents the utilization of CA – due to its solubility properties – required a polar type of solvent. Preliminary testing showed that DMSO could be employed to bring the template in solution with the monomers mentioned before, and therefore it was chosen as porogen. DMSO is a polar aprotic solvent depicting an intermediate value for dielectric constants and polarity; this would prevent the porogen to interfere with the template-monomer(s) interaction(s). Fig. 2 shows the interaction of carminic acid (template) with 4Vpy, a monomer utilized in this study. The energy difference between the orientation shown in Fig. 2 and any other possible orientation (N of pyridine interaction with the hydroxyl of carminic acid) was −8.56 kcal, indicating that hydrogen bonding is the most favorable interaction.

Table 1 shows the MIP materials obtained by utilizing MAA and/or 4Vpy as monomers and EGDMA as a cross-linker. The template: monomer: cross-linker ratio selected was 1: 5: 40. This ratio has been used extensively in imprinting to ensure sufficient amount of binding points and mechanical strength to retain binding memory. As expected, a rigid polymer was formed, which was ground

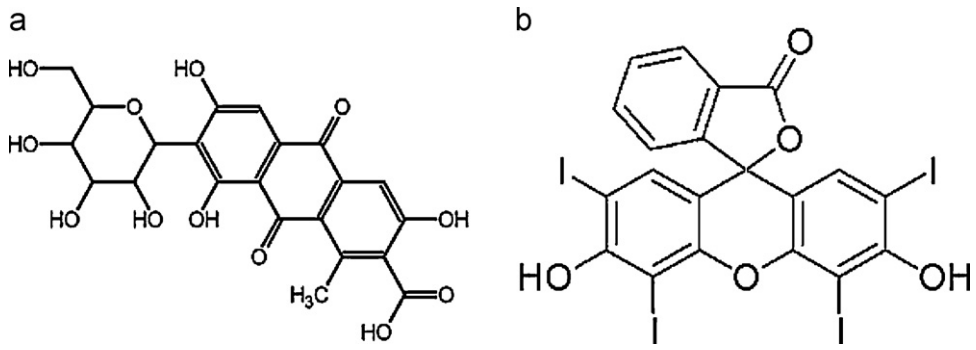

Fig. 1. Structure of carminic acid (a) and its structural analog (Erythrosine B) (b). The Erythrosine B is a food dye as well.

Table 1
List of reagents and conditions used in the synthesis of polymer materials.

Polymer code	Polymer	Template	Monomer	Cross-linker	C/M
M_{NIP}	NIP (MAA)	–	MAA	EGDMA	5:1
M_{MIP}	MIP (MAA)	CA	MAA	EGDMA	5:1
MV_{NIP}	NIP(MAA,4Vpy)	–	MAA,4Vpy	EGDMA	5: (0.5,0.5)
MV_{MIP}	MIP(MAA,4Vpy)	CA	MAA,4Vpy	EGDMA	5: (0.5,0.5)
V_{NIP}	NIP (4Vpy)	–	4Vpy	EGDMA	5:1
V_{MIP}	MIP (4Vpy)	CA	4Vpy	EGDMA	5:1

DMSO was used as porogen and AIBN as initiator. The synthesis was performed at 60 °C. C/M is the ratio of cross linker and monomer.

and sieved into 45–75 μm (irregular) particles. By leaching the template dye from the matrix, a molecularly imprinted polymer was generated.

4.2. Physical characterization of V_{MIP} particles

Porosity and surface area of V_{MIP} was determined by conventional adsorption/desorption measurements, using the Brauner–Emmer–Teller (BET) multipoint method. This method is considered the specific for mesoporous materials as for the conventional resins having a surface area less than 0.1 m^2/g is not possible to characterize by this method but later on Bae et al. proved it a suitable method for conventional resins [19,20]. Table 2 summarizes the structural characteristics and its comparison with others.

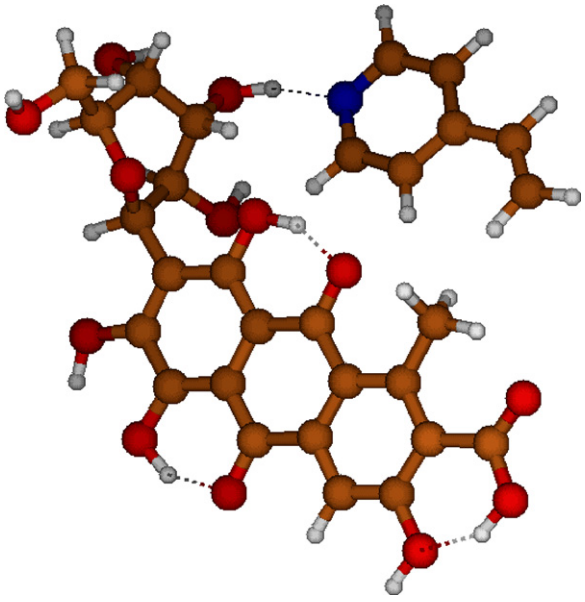

Fig. 2. Computer simulation showing the interaction of monomer (vinyl pyridine) and template (carminic acid)during MIP synthesis, the medium was considered gas for simulation.

The pore diameter was 14 nm; the average surface area for the obtained MIP particles was 292 m^2/g while the total pore volume reached 0.49 cm^3/g. The larger pore diameter in combination with higher pore volumes and high surface area reveals that the cavities are present in the material under study. The pore size is well within the mesoporous range (2.0–25 nm) and is supposed to allow the easy diffusion of template to the specific cavity created by the template. Table 2 shows the comparison of the studied material with other porous particles and some ion exchange materials. The porous material labeled as TBT is having the pore size in the same range, comparatively lower pore volume and surface area [21]. The higher surface area is responsible for higher capacities as well. The X1-A material synthesized by precipitation approach shows higher pore diameter and surface area as compared to commercial resins; which are mesoporous but the pore diameter and the surface area is comparatively less as described by Kun at al., the same trend was observed by Huang et al. [22,23]. The high pore volume and larger surface area of the MIP studies here is because of embedding of template molecule and cavity after removal of this template

The particle zeta potential of V_{MIP} was determined in a 50 mM ammonium acetate buffer (pH 4) and in 20 mM phosphate buffer (pH 7). MIP particles were charged positively at pH 4 (+11.6 mV) and negatively at pH 7 (−18.9 mV). This behavior was expected because the 4Vyp having pK_a of 5.2 should be positively charged at pH 4 and negatively charged at pH 7. The possible interaction at pH 4 was because of the opposite net charge at MIP (positive) and template (negative), the charge is same in the case of pH 7 (both negative). The high values for zeta potentials also suggest that a suspension of MIP particles would be moderately stable, and therefore such

Table 2
Summary of physical and structural properties of V_{MIP} and related compounds.

	Pore size (nm)	Surface area (m^2/g)	Pore volume (cm^3/g)
V_{MIP} (this report)	14	292	0.49
TBT particles [21]	10–14	115–134	0.2
X1-A particles [22]	24	383	0.88
IR-15 [22]	8	55	0.36
IRC 50 [22]	80	1.8	0.152
IR-120 [22]	–	<0.1	0.018

particles will have a low tendency to aggregate. This could be an advantage for the utilization of the MIP particles as adsorbents in a finite bath system.

4.3. Functional screening of MIP materials

Recognition experiments were run in order to select functional materials having the ability to capture carminic acid from a watery medium. The sorption performance of the three types of MIP particles synthesized toward the template was evaluated in aqueous environment to simulate the conditions prevailing during industrial processing. For comparison, commercial resin beads (taken as positive and negative controls) as well as NIP particles were introduced. From Fig. 3, it can be observed that all the three materials (M_{MIP}, MV_{MIP} and V_{MIP}) depict binding properties although the polymer containing 4Vpy (V_{MIP}) was able to capture a much higher amount of the template from solution. The latter has shown a percentage binding and recovery, which is comparable to Amberlite-IRA, an anion exchange utilized as a positive control. The Amberlite-IRA is shown to bind strongly to CA because of ionic and hydrophobic interactions [6]. Fig. 3 depicts the binding and recovery of MIPs or the control in the presence of low concentrations of substrate (200 μl CA of 1 mg/ml). Moreover, the V_{MIP} also showed a highly reversible interaction with the template, which was not the case for the other imprinted materials.

The high recoveries for the V_{MIP} particles can be partially attributed to the presence of protonated nitrogen atoms within the structure of vinyl pyridine, employed as a monomer during synthesis. At the working pH of the screening assay, carminic acid would be negatively charged therefore, ionic interactions could be postulated as an important mechanism for template recognition. However, the difference in the recoveries of V_{MIP} (95%) and V_{NIP} (23%) is clear indication of an imprinting effect beyond a pure Coulomb-type (charge mediated) interaction. A pure ionic interaction, however, may be fully responsible for carminic acid binding onto the control particles.

The imprinted M_{MIP} and MV_{MIP} showed a clear recognition behavior as seen from the comparison with their non-imprinted counterparts. Unfortunately, these materials presented low binding capacity values and therefore deliver low yields e.g. below 5%. Recognition would have been mediated more likely by hydrogen bonding in this case. Polymers for bile salts were synthesized by Yañez et al.; using different monomers and declare; that as hydrogen bonding is not favorable in aqueous medium, the polymer can bind fewer templates as compared to the polymer with electrostatic interaction [24]. Another imprinted polymer for water soluble peptide was synthesized by Rachkov et al. declared that the selectivity of the template is attributed to electrostatic interaction while specificity to hydrogen bonding and hydrophobic interaction.

Although it is known that MIPs generally express better recognition abilities toward the target molecule when the binding is carried out using the same porogen that was used for synthesis [25], all the imprinted material tested here conserved a degree of template recognition (and binding ability) even when tested in water as oppose to DMSO. The V_{MIP} and V_{NIP} were selected for further characterization and evaluation.

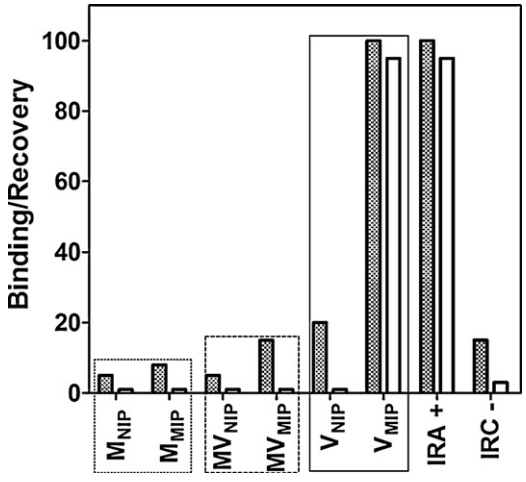

Fig. 3. Primary evaluation of polymer materials synthesized using different monomers. Aqueous solution of CA 1 mg/ml, pH 4 was used for evaluation. The dye was recovered by 0.5 M NaOH solution in water. Negative and positive controls are shown for comparison. CA concentration was determined by absorbance at 494 nm in 0.2 N HCl Filled bars representing the bindings and empty bars showing the recoveries.

4.4. Equilibrium adsorption characteristics

4.4.1. Adsorption isotherm

An adsorption isotherm is a measure of the relationship between the concentrations of adsorbed and free template at equilibrium. The adsorption of dyes on various types of solid particles is usually well modeled by the Redlich–Peterson equation or the Langmuir expression [4]. Since the imprinted materials synthesized in this work were obtained via the non-covalent approach, it might be expected; to depict a degree of heterogeneity within the available binding sites. Under such circumstances, the adsorption characteristics of a (heterogeneous) material can be better represented by the Langmuir–Freundlich isotherm [13,15]. This so-called Sip's equation has three parameters, which allows a representation of both high-affinity and low-affinity binding sites.

Fig. 4 depicts the adsorption behavior of carminic acid onto V_{MIP} particles in comparison with the V_{NIP}. An important parameter for the technological utilization of an adsorbent is the capacity it depicts toward a targeted product. In this case, the imprinted particles (V_{MIP}) reached a maximum capacity of 316 mg/g (0.64 mmol/g), dramatically higher than observed for the non-imprinted adsorbent; 1.4 mg/g (0.0064 mmol/g). This is surprising since the capacity values of MIPs synthesized by the non-covalent approach are frequently low (e.g. within the range 0.1–3.5 mg/g) and usually there is no much difference between imprinted and non-imprinted polymers in this regard [26–28]. Moreover, a few reports indicate the possibility of increasing total binding capacity values for MIP materials (e.g. into the 300 mg/g range) but a concomitant increase in binding capacity values for the NIP counterparts was

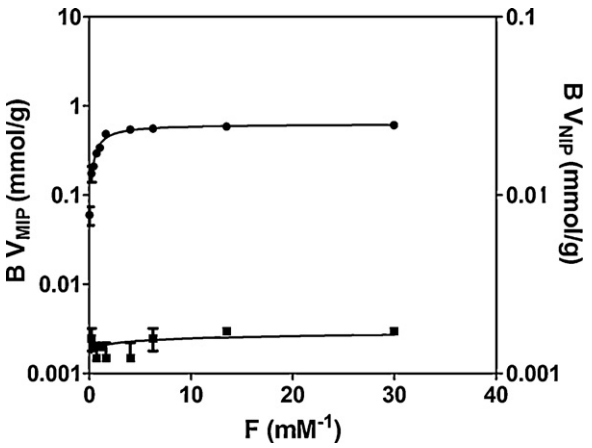

Fig. 4. Adsorption isotherm of CA on the polymeric imprinted material and non-imprinted. CA (4–40 mg/g in the water having pH 4) was applied for 16 h. CA concentration was determined by absorbance at 494 nm in 0.2 N HCl. The circles showing the V_{MIP} and squares are V_{NIP}.

Table 3
Fitting parameters for Langmuir–Freundlich isotherms applied to V_{MIP} and V_{NIP}.

	N_t (mmol/g)	α (mM)	m	R^2
V_{MIP}	0.64	1.4	1	0.98
V_{NIP}	0.0064	0.5	0.17	0.99

also observed (e.g. in the 200+ mg/g range) [18,29]. The covalent imprinting approach tends to deliver a greater difference between the capacity values for the imprinted and non-imprinted materials [30].

The parameters calculated from the model are summarized in Table 3 (R^2 = 0.98). In the case of the V_{MIP} particles, the heterogeneity index (m) was approximately close to 1, indicating the presence of highly homogeneous binding sites. On the other hand, the V_{NIP} particles presented more heterogeneity (m = 0.17) and extremely low affinity i.e. 100 times less than the MIP. The median binding affinity values found were (K_0) 1.4 mM^{-1} and 0.0072 mM^{-1} for the imprinted and the non-imprinted material, respectively. This indicated a very strong interaction of the template with the V_{MIP} but not with the V_{NIP} particles. These parameters are in accordance with other studies [13].

4.4.2. Affinity-site distribution

The binding properties always cannot be extrapolated from the fitting coefficients of isotherm; the affinity distribution can still predict a relatively accurate and quantitative measure of binding properties [31]. The affinity distribution of a material can be represented by plotting the number of binding sites versus the logarithmic value of the corresponding association constants; this yields the distribution of sites over a continuous range binding constants. The affinity distribution characterizes the heterogeneity of the material as well. Eq. (2) when employed with the Langmuir–Freundlich equation as a fitting model, allowed the calculation of the numbers of binding sites at respective association constant. Fig. 5 depicts the affinity distribution functions for V_{MIP} and V_{NIP}. The profile of the affinity distribution of molecularly imprinted polymer was Gaussian and narrow, giving the highest binding sites (N = 1.8 mmol/g) at log K of 0.15 (K = 1.5). In comparison, the non-imprinted polymer showed the maximum binding sites (N = 0.005 mmol/g) at log K of −1.5 (K = 0.03). For V_{NIP} a continuous decrease in binding site number can be observed when the values of the association constant increased. These results are comparable with other reports. It is usually observed that when the value of the association constant decreases the recognition ability of the polymers toward template is lost (exponential decrease) [15].

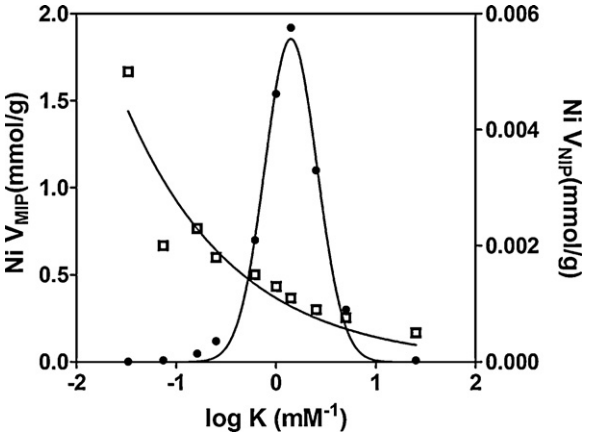

Fig. 5. Affinity distribution functions for V_{MIP} circles and V_{NIP} squares. The affinity distribution function was calculated by using Eq. (3); by using the Langmuir–Freundlich isotherm parameter.

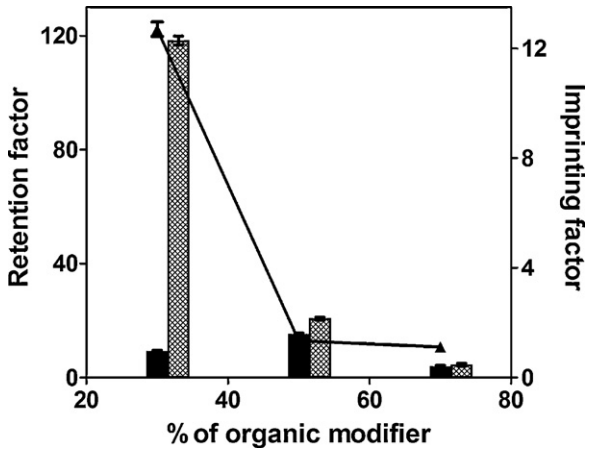

Fig. 6. Retention factor (bar graph) and imprinting factor (line graph) determined at different percentages of organic modifier. The shaded bar is showing the retention of CA on V_{MIP} and close bar are retention on V_{NIP}.

4.5. Selectivity of MIP particles toward carminic acid

The recognition properties of the MIP material were also evaluated by liquid chromatographic experiments. V_{MIP} and V_{NIP} particles were packed in a PEEK column, which was mounted in a HPLC system. In order to assess the strength of interaction of the template (carminic acid) with the mentioned materials; the retention times were recorded as a function of the composition of the mobile phase e.g. the content of organic modifier. Experiments were run at pH 4 and with a buffer of low conductivity (4.0 mS/cm) to allow for ionic interaction between the materials. V_{MIP} and V_{NIP} materials were depicted a very similar chromatographic behavior at higher concentration of organic modifier, as depicted from the retention factor values; shown in Fig. 6. On the contrary, a significant difference between the retention times was observed upon increasing the polarity of the mobile phase e.g. at 30% organic modifier content, chromatogram shown in Fig. 7. Wide range of buffer combination (organic and inorganic) was used to visualize the difference in retention times of the two materials (MIP and NIP), which actually will be the result of imprinting. If the template and material prefer to have ionic interaction in aqueous media, they will show the difference in retention times in higher organic buffers and if

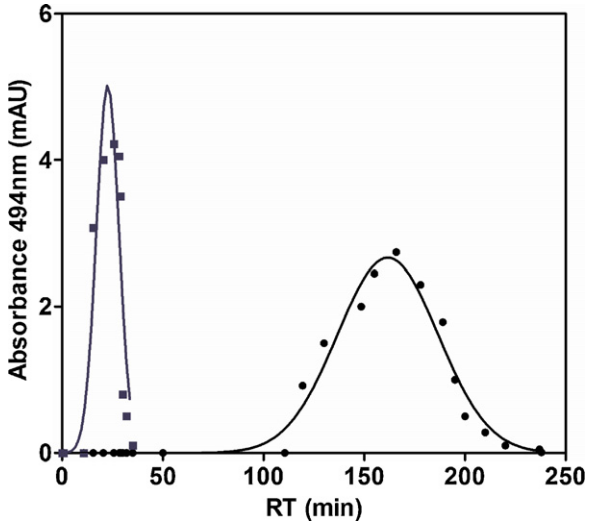

Fig. 7. Chromatogram shows the retention of carminic acid on V_{MIP} (circles) and V_{NIP} (squares). Mobile phase was 30% of organic modifier and 70% of acetate buffer pH 4. The sample was 1 mg/ml CA (200 μl) and flow rate of 1 ml/min.

the interaction results of the hydrophobic characteristics, the difference in retention times will appear in lower organic modifiers as seen in this case. Under such conditions, the retention factor for V_{MIP} was 110 while for V_{NIP} was 5.4. These (retention factor) are the retention time values normalized by retention time of non-retained solute (calculated by Eq. (6)). This allowed the calculation of an imprinting factor (I_f) equal to 13. This may indicate that hydrophobic interactions could play a role in binding of the template by the imprinted material. Additional phenomena may occur, for example $\pi-\pi$ stacking and electrostatic interaction, that is relatively common within dye molecules.

The selectivity factor for the V_{MIP} was determined, similar chromatographic conditions were applied for both the template and the analog (Erythrosine B); the content of the organic modifier was kept at 30%. Selectivity factor equal to 15 was observed; indicative of an excellent imprinting effect; other reports have informed selectivity ratios within the range 4.5–6.4 [32].

Taken as a whole, the values for both imprinting factor (V_{MIP} = 13) and selectivity factor (V_{MIP} = 15) are indicative of a material with potentially good performance for the selective sequestration of carminic acid from a crude feedstock.

4.6. Evaluation of MIP particles for direct carminic acid recovery in a finite bath

Crushed cochineal was extracted with a hot alkaline solution to render a crude preparation containing carminic acid at a concentration of 8.0–10 kg/m^3. The crude extract also contained proteins ($\leq$0.25 kg/m^3), had a pH $\approx$ 5 and conductivity $\approx$4 mS/cm. It was observed that the crude extract presented an increased viscosity upon cooling and that it offered resistance to conventional filtration. This may be responsible for lower recovery yields during traditional processing, which usually rely on several precipitation and filtration steps [33]. It has been reported, that being an insect-derived substance, the cochineal extracts may contain allergenic contaminant proteins. An adsorption-based process is able to remove such components and improve the quality and safety of the final product [34].

The effect of time on CA adsorption was analyzed by using a kinetic rate constant model (Eq. (3)). The normalized concentration (C/C_o) was plotted against time. According to Eq. (3), the negative slope of the equation shows that the adsorbed template should increase with the effect of time. If maximum contact time was given, till establish equilibrium, this study can give the maximum capacity and dissociation constant values, as observed in static study. Finite bath is the most common approach to study the dynamic behavior of non-porous particles. As we can see from Eq. (3) that the decrease in concentration is related to negative kinematic viscosity and stirring is the sheer force applied that can change the kinematic viscosity of non-Newtonian fluids (solid suspension). The decrease in kinematic viscosity will increase the binding of the template. Fig. 8 shows the effect of stirrer speed on CA adsorption, the increase in stirrer speed increase the rate of adsorption, attributed to better suspension, mixing of particles and mass transfer improvement. Other authors undertook a similar approach. The kinetic rate constant value was 1.5×10^{-5} ml/mg/s. This can be compared with other suspensions of small particles [35,36]. The data presented in Fig. 8 confirm that approximately 90% of the template bind within a processing time of 24 min, a fact that also indicate the presence of sites with high affinity and sufficient capacity. Mixing into the transition regime has provoked a much faster mass transfer which resulted in a much shorten processing time and therefore, an increase in productivity. Other authors have reported on the relationship between rapid product uptake and binding site density [37].

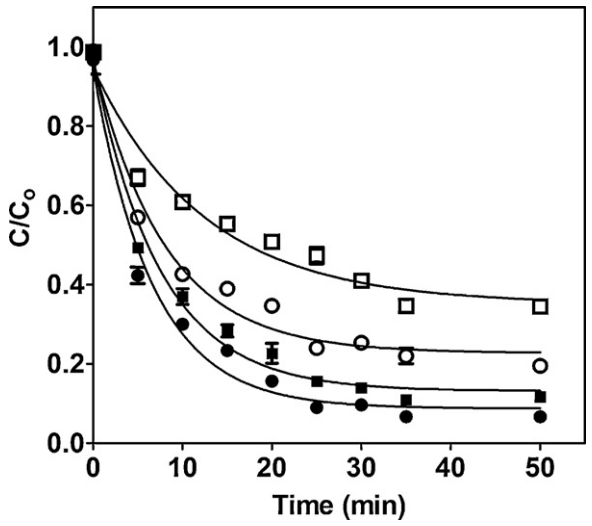

Fig. 8. Effect of stirrer speed at a CA adsorption rate on V_{MIP}, solid lines shows the fitting of experimental data (points) to the non-linear regression analysis. The stirrer speeds are as follows; (□) 56 rpm, (○) 156 rpm, (■) 256 rpm, (●) 356 rpm.

5. Conclusions

Natural products are of utmost importance nowadays due to strong consumer preference. The production of carminic acid, a natural red dye, usually requires a complicated extraction and purification scheme. Molecularly imprinted polymer particles were introduced to facilitate the capture of the mentioned dye directly from a crude cochineal extract. It was observed the V_{MIP} presented excellent characteristic as a potential industrial adsorbent.

The adsorption system was well described utilizing the Langmuir–Freundlich isotherm, which indicated the presence of highly homogeneous binding sites. The imprinting effect was further confirmed by the affinity distribution (imprinting factor = 13). Chromatographic experiment with a structural analog indicated high selectivity (selectivity factor = 15).

Finite bath experiments run with crude cochineal indicated the feasibility of the imprinted material for efficient capture of the product. Moreover, introducing mechanical stirring under predetermined conditions increased productivity due to mass transfer effects. This study can assist in the downstream processing of carminic acid.

Acknowledgements

Noor Shad Bibi thank the Higher Education Commission of Pakistan for financial support. Mariano Grasselli and Marcelo Fernández-Lahore are members of the Consejo Nacional de Investigaciones Cientificas (CONICET, Buenos Aires, Argentina). This work has been partially supported be the European Commission under the Project FP7-SME-2007-1 ELECTROEXTRACTION 222220 and BMBF-ERA-Bet PGSYS 513050290.

References

[1] Tateo F, Bononi M. Fast determination of Sudan I by HPLC/APCI-MS in hot chilli, spices, and oven-baked foods. J Agric Food Chem 2004;52:655–8.
[2] Long C, Mai Z, Yang Y, Zhu B, Xu X, Lu L, Zou X. Synthesis and characterization of a novel molecularly imprinted polymer for simultaneous extraction and determination of water-soluble and fat-soluble synthetic colorants in chilli products by solid phase extraction and high performance liquid chromatography. J Chromatogr A 2009;1216:8379–85.
[3] Lancaster FE, Lawrence JF. High-performance liquid chromatographic separation of carminic acid, α- and β-bixin, and α- and β-norbixin, and the determination of carminic acid in foods. J Chromatogr A 1996;732:394–8.

[4] Cabrera RB, Fernandez-Lahore HM. Primary recovery of acid food colorant. Int J Food Sci Technol 2007;42:1315–26.
[5] Maier MS, Parera SD, Seldes AM. Matrix-assisted laser desorption and electrospray ionization mass spectrometry of carminic acid isolated from cochineal. Int J Mass Spectrom 2004;232:225–9.
[6] Cabrera RB, Fernandez-Lahore H. Sorption characteristics and performance of an acid dye on a gel-type weak anion exchanger in a finite bath. J Sci Food Agric 2006;86:2318–26.
[7] Pichon V, Bouzige M, Miège C, Hennion M. Immunosorbents: natural molecular recognition materials for sample preparation of complex environmental matrices. TrAC Trends Anal Chem 1999;18:219–35.
[8] Huiting Z, Tao S, Fulin Z, Tiechun C, Synthesis Canping P. Characterization of molecularly imprinted polymers for phenoxyacetic acids. Int J Mol Sci 2008;9:98–106.
[9] Wulff G, Sarhan A. Ãœber die anwendung von enzymanalog gebauten polymeren zur racemattrennung. Ang Chem 1972;84:364.
[10] Arshady R, Mosbach K. Synthesis of substrate-selective polymers by host–guest polymerization. Macromol Chem 1981;182:687–92.
[11] Song S, Shi X, Li R, Lin Z, Wu A, Zhang D. Extraction of chlorpromazine with a new molecularly imprinted polymer from pig urine. Process Biochem 2008;43:1209–14.
[12] Robert S. On the structure of a catalyst surface II. J Chem Phys 1950;18:1024–6.
[13] Umpleby RJ, Baxter SC, Chen Y, Shah RN, Shimizu KD. Characterization of molecularly imprinted polymers with the Langmuir–Freundlich isotherm. Anal Chem 2001;73:4584–91.
[14] Pérez Cordoves AI, Granda Valdés M, Torres Fernández JC, Pina Luis G, García-Calzón JA, Díaz García ME. Characterization of the binding site affinity distribution of a surfactant-modified clinoptilolite. Micropor Mesopor Mater 2008;109:38–48.
[15] Stanley BJ, Szabelski P, Chen Y, Sellergren B, Guiochon G. Affinity Distributions of a molecularly imprinted polymer calculated numerically by the expectation-maximization method. Langmuir 2003;19:772–8.
[16] Ottewill RH, Shaw JN. Electrophoretic studies on polystyrene lattices. J Electroanal Chem Inter Electrochem 1972;37:133–42.
[17] Umpleby RJ, Baxter SC, Rampey AM, Rushton GT, Chen Y, Shimizu KD. Characterization of the heterogeneous binding site affinity distributions in molecularly imprinted polymers. J Chromatogr B 2004;804:141–9.
[18] Al-Degs Y, Abu-Surrah A, Ibrahim K. Preparation of highly selective solid-phase extractants for Cibacron reactive dyes using molecularly imprinted polymers. Anal Bioanal Chem 2009;393:1055–62.
[19] Kunin R, Meitzner EA, Oline JA, Fisher SA, Frisch N. Characterization of amberlyst 15. Macroreticular sulfonic acid cation exchange resin. I&EC Prod Res Dev 1962;1:140–4.
[20] Bae Y, YazaydÄ±n AO, Snurr RQ. Evaluation of the BET Method for determining surface areas of MOFs and zeolites that contain ultra-micropores. Langmuir 2010;26:5475–83.
[21] Liu K, Zhang M, Shi K, Fu H. Large-pore mesoporous nanocrystalline titania thin films synthesized through evaporation-induced self-assembly. Mater Lett 2005;59:3308–10.
[22] Kun KA, Kunin R. The pore structure of macroreticular ion exchange resins. J Polym Sci Part C: Polym Symp 1967;16:1457–69.
[23] Huang M, Chou C, Teng H. Pore-size effects on activated-carbon capacities for volatile organic compound adsorption. AIChE J 2002;48:1804–10.
[24] Yañez F, Chianella I, Piletsky SA, Concheiro A, Alvarez-Lorenzo C. Computational modeling and molecular imprinting for the development of acrylic polymers with high affinity for bile salts. Anal Chim Acta 2010;659:178–85.
[25] Chassaing C, Stokes J, Venn RF, Lanza F, Sellergren B, Holmberg A, Berggren C. Molecularly imprinted polymers for the determination of a pharmaceutical development compound in plasma using 96-well MISPE technology. J Chromatogr B 2004;804:71–81.
[26] Singh D, Mishra S. Synthesis of a new Cu(II)-ion imprinted polymer for solid phase extraction and preconcentration of Cu(II). Chromatographia 2009;70:1539–45.
[27] Chen L, Liu J, Zeng Q, Wang H, Yu A, Zhang H, Ding L. Preparation of magnetic molecularly imprinted polymer for the separation of tetracycline antibiotics from egg and tissue samples. J Chromatogr A 2009;1216:3710–9.
[28] Duy SV, Lefebvre-Tournier I, Pichon V, Hugon-Chapuis F, Puy J-, Périgaud C. Molecularly imprinted polymer for analysis of zidovudine and stavudine in human serum by liquid chromatography–mass spectrometry. J Chromatogr B 2009;877:1101–8.
[29] Feng Q, Zhao L, Lin J. Molecularly imprinted polymer as micro-solid phase extraction combined with high performance liquid chromatography to determine phenolic compounds in environmental water samples. Anal Chim Acta 2009;650:70–6.
[30] Monier M, El-Sokkary AMA. Preparation of molecularly imprinted cross-linked chitosan/glutaraldehyde resin for enantioselective separation of L-glutamic acid. Int J Biol Macromol 2010;47:207–13.
[31] Rampey AM, Umpleby RJ, Rushton GT, Iseman JC, Shah RN, Shimizu KD. Characterization of the imprint effect and the influence of imprinting conditions on affinity, capacity, and heterogeneity in molecularly imprinted polymers using the Freundlich isotherm-affinity distribution analysis. Anal Chem 2004;76:1123–33.
[32] Cacho C, Turiel E, Pérez-Conde C. Molecularly imprinted polymers: an analytical tool for the determination of benzimidazole compounds in water samples. Talanta 2009;78:1029–35.
[33] Ziegler R, Engler DL, Bartnek F, Antwerpen RV, Bluestein HA, Gilkey JC, Yepiz-Plascencia G. A new type of highly polymerized yolk protein from the cochineal insect *Dactylopius confusus*. Arch Insect Biochem Physiol 1996;31:273–87.
[34] Ichi T, Koda T, Yukawa C, Sakata M, Sato H. Purified cochineal and method for its production 2007; 10/428995:1–12.
[35] Skidmore GL, Hortsmann BJ, Chase HA. Modelling single-component protein adsorption to the cation exchanger s sepharose® FF. J Chromatogr A 1990;498:113–28.
[36] Fernandez MA, Carta G. Characterization of protein adsorption by composite silica–polyacrylamide gel anion exchangers. I. Equilibrium and mass transfer in agitated contactors. J Chromatogr A 1996;746:169–83.
[37] Corton E, García-Calzón JA, Díaz-García ME. Kinetics and binding properties of cloramphenicol imprinted polymers. J Non-Cryst Solids 2007;353:974–80.